Network patterns and strength of orbital currents in layered cuprates

M. V. Eremin,[1] I. Eremin,[1,2] and A. Terzi[1]
[1]*Physics Department, Kazan State University, 420008 Kazan, Russia*
[2]*Institut für Theoretische Physik, Freie Universität Berlin, D-14195 Berlin, Germany*
(Received 18 July 2002; published 30 September 2002)

In the frame of the *t-J-G* model we derive a microscopical expression for circulating orbital currents in layered cuprates using the anomalous correlation functions. In agreement with muon spin relaxation, nuclear quadrupolar resonance and neutron scattering (NS) experiments in $YBa_2Cu_3O_{6+x}$ we successfully explain the order of magnitude and the monotonous increase of the *internal* magnetic fields resulting from these currents upon cooling. However, the marked enhancement of NS intensity at T_c, reported recently, seems to indicate a non-mean-field feature of coexistence between the current and superconducting states. A relation of this enhancement to the appearance of a small admixture of *s*-wave symmetry component of the conventional charge-density wave state and also the dependence of the sliding charge-current condensation energy on the phase of the order parameter are discussed.

DOI: 10.1103/PhysRevB.66.104524 PACS number(s): 74.72.−h, 74.20.Mn, 74.25.Ha

A possibility for a staggered orbital current phase formation in layered cuprates has attracted much interest recently.[1–11] Remarkably, it was shown that most of the observed properties referred to as a so-called pseudogap phenomenon can be naturally explained in an extended charge-density wave (CDW) scenario with a complex order parameter (shortly $s+id$-CDW) in underdoped cuprates. The real *s*-wave symmetry component corresponds to the formation of conventional charge- (or spin) density waves whereas the imaginary part of the order parameter has a $d_{x^2-y^2}$-wave symmetry and corresponds to a staggered current phase. A different kind of experiments can be interpreted in favor of the staggered orbital current phase such as the observation of orbital antiferromagnetism in $YBa_2Cu_3O_{6+y}$ by means of neutron scattering(NS) experiments reported in Refs. 5, 6 and zero-field muon spin relaxation (μSR) experiments.[8] Moreover, recent investigations using nuclear magnetic resonance (NMR) indicate the presence of internal fluctuating magnetic fields in the superconducting state of layered cuprates.[9–11] Most importantly, the observed enhancement of the magnetic moment's intensity at T_c (Refs. 5, 6) seems to indicate an intrinsic and nontrivial relation between the superconducting and the pseudogap phases. In this context a microscopical analysis of the network patterns and the strength of orbital currents becomes very actual.

In general, the possibility of $s+id$-CDW phase formation is related to a divergence of the dynamical charge susceptibility at the wave vector $\mathbf{Q}_i \approx (\pi,\pi)$ in the first Brillouin zone and it was demonstrated recently for cuprates.[12] In this report we derive the analytical expression for the current flow and show how its orbital network pattern can be reconstructed. Most importantly, we calculate the intensity of the resulting internal magnetic fields and the corresponding orbital magnetic moments. We find that its enhancement at T_c may result from the presence of a relatively small *s*-wave component in the extended CDW. The latter agrees well with the observation of the increase of the nuclear quadrupole resonance (NQR) linewidth at the Cu(2) site (see, Ref. 11). In addition, the non-mean-field character of the coexistence of superconductivity and $s+id$-CDW phases has to be taken into account.

Hamiltonian and general expression for the current flow. In our analysis we start from the following *t-J-G* model Hamiltonian:

$$H=\sum_{ij} t_{ij}\Psi_i^{pd,\sigma}\Psi_j^{\sigma,pd}+\sum_{i>j} J_{ij}\left[(\mathbf{S}_i\mathbf{S}_j)-\frac{n_i n_j}{4}\right] + \sum_{i>j} G_{ij}\delta_i\delta_j, \tag{1}$$

where $\Psi_i^{\alpha,\beta}=|i,\alpha\rangle\langle i,\beta|$ are projecting Hubbard-like operators. The index pd corresponds to a Zhang-Rice singlet formation with one hole placed on the copper site, whereas the second hole is distributed on the neighboring oxygen sites.[13] Here, t_{ij} is a hopping integral, J_{ij} is a superexchange coupling parameter of the copper spins, and $\sigma=\pm 1/2$. $\delta_i=\Psi_i^{pd,dp}$ is a hole doping operator. The anticommutator relations are given by $P_{pd}=[\Psi_i^{\uparrow,pd}\Psi_i^{pd,\uparrow}]=(2+\delta_i)/4+s_i^z$, where s_i^z is a spin operator. As in Ref. 12 we also use the parameter of a screened Coulomb repulsion of the doped holes at different sites, G_{ij}. The quasiparticle energy dispersion and the correlation functions were calculated in a Roth-type decoupling scheme for the Green's functions.[14,15]

Let us first consider the equation of motion for the Fourier transform of the ''spin-up'' operator

$$(\omega-\epsilon_{\mathbf{k}}^{\uparrow})\Psi_{\mathbf{k}}^{\uparrow,pd}=\eta_{\mathbf{k},\mathbf{Q}}^{\uparrow}\Psi_{\mathbf{k}+\mathbf{Q}}^{\uparrow,pd}+\Delta_{\mathbf{k}}\Psi_{-\mathbf{k}}^{pd,\downarrow}+U_{\mathbf{k},\mathbf{Q}}^{\uparrow}\Psi_{-\mathbf{k}-\mathbf{Q}}^{pd,\downarrow}, \tag{2}$$

where $\Delta_{\mathbf{k}}$ and $U_{\mathbf{k},\mathbf{Q}}$ correspond to the uniform and nonuniform superconducting states, respectively. Three other equations can be obtained by simple substitution of $\mathbf{k}\rightarrow\mathbf{k}+\mathbf{Q}$, $\mathbf{Q}\rightarrow-\mathbf{Q}$ and also by complex conjugation. In addition, four similar equations for the ''spin-down'' operator are assumed. The order parameter $\eta_{\mathbf{k},\mathbf{Q}}^{\uparrow}$, which is the most interesting for us, describes the formation of a superstructure pattern such as charge-density and spin-density (SDW) waves. Starting from Eq. (1) one arrives to the following equation:

$$\eta^{\uparrow}_{\mathbf{k},\mathbf{Q}} = -\frac{1}{2NP_{pd}} \sum_{\mathbf{k}'} [J_{\mathbf{k}'-\mathbf{k}} \langle \Psi^{pd,\downarrow}_{\mathbf{k}'+\mathbf{Q}} \Psi^{\downarrow,pd}_{\mathbf{k}'} \rangle + 2G_{\mathbf{k}'-\mathbf{k}} \langle \Psi^{pd,\uparrow}_{\mathbf{k}'+\mathbf{Q}} \Psi^{\uparrow,pd}_{\mathbf{k}'} \rangle], \quad (3)$$

where the correlation functions $\langle \Psi^{pd,\uparrow}_{\mathbf{k}'+\mathbf{Q}} \Psi^{\uparrow,pd}_{\mathbf{k}'} \rangle$ and $\langle \Psi^{pd,\downarrow}_{\mathbf{k}'+\mathbf{Q}} \Psi^{\downarrow,pd}_{\mathbf{k}'} \rangle$ are expressed via the order parameters $\eta^{\uparrow}_{\mathbf{k},\mathbf{Q}}$, $\Delta_{\mathbf{k}}$, and $U^{\uparrow}_{\mathbf{k},\mathbf{Q}}$. The latter order parameter that describes the formation of the nonuniform superconducting state will be discussed later. The Fourier transform of the intersite Coulomb repulsion on the square lattice reads

$$G_{\mathbf{q}} = 2G_1(\cos q_x + \cos q_y) + 4G_2 \cos q_x \cos q_y + \cdots, \quad (4)$$

where G_1 and G_2 refer to the nearest- and next-nearest-neighbor sites on the lattice. The same holds for the superexchange interaction. Substituting these Fourier transformations into Eq. (3) one gets that the $\mathbf{k}$ dependence of the CDW/SDW-order parameter is

$$\eta^{\uparrow}_{\mathbf{k},\mathbf{Q}} = d^{\uparrow}_x(\mathbf{Q}) \cos k_x + d^{\uparrow}_y(\mathbf{Q}) \cos k_y + s^{\uparrow}(\mathbf{Q}) \cos k_x \cos k_y + \cdots. \quad (5)$$

Taking into account that $(\eta^{\uparrow}_{\mathbf{k}+\mathbf{Q},-\mathbf{Q}})^* = \eta^{\uparrow}_{\mathbf{k},\mathbf{Q}}$ one clearly sees that the d_x and d_y components are imaginary (id-CDW or so-called d-density wave in terms of Ref. 1), while the s-wave component remains real (conventional CDW-state). Since the symmetries of both states are different, the real and imaginary part of Eq. (3) decouple. In general, this yields $s+id$-CDW state

$$\frac{1}{2}(\eta^{\uparrow}_{\mathbf{k},\mathbf{Q}} + \eta^{\downarrow}_{\mathbf{k},\mathbf{Q}}) = \eta_{\mathbf{k}}(T) = s(T) + id(T)(\cos k_x - \cos k_y), \quad (6)$$

where we assume that $\eta^{\uparrow}_{\mathbf{k},\mathbf{Q}} - \eta^{\downarrow}_{\mathbf{k},\mathbf{Q}} = 0$. Note, the deviation of the momentum dependence of CDW order parameter from the pure $(\cos k_x - \cos k_y)$ behavior can be clearly seen from ARPES experiments.[16] Moreover, from Fig. 2 of Ref. 16 one estimates $s(T)/d(T) \sim 0.05$, which also follows from our Eq. (1) due to $J_1 + 2G_1 > J_2 + 2G_2$.

The network patterns and the strength of the orbital currents can be obtained using the charge conservation law

$$\frac{\partial}{\partial t} \int \rho dV = \int \mathbf{j}\, \mathbf{dS}. \quad (7)$$

The operator of the fluctuating charge per unit cell with number i is given by

$$e\Psi^{pd,pd}_i = e\,\delta_i = \tilde{\delta}_i. \quad (8)$$

It obeys the equation of motion

$$i\hbar \frac{\partial}{\partial t} \tilde{\delta}_i = [\tilde{\delta}_i, H]. \quad (9)$$

Calculating the commutator with our Hamiltonian (1) we arrive to the following expression:

$$i\hbar \frac{\partial}{\partial t} \tilde{\delta}_i = e \sum t_{ij} \Psi^{pd,\sigma}_i \Psi^{\sigma,pd}_j - e \sum t_{ji} \Psi^{pd,\sigma}_j \Psi^{\sigma,pd}_i, \quad (10)$$

where the right-hand side of this equation is a current operator. In order to calculate its thermodynamic value along the link $\langle ij \rangle$ we make the Fourier transform of Eq. (10). Then, the probability of hopping from site i to j can be written as

$$\langle \Psi^{pd,\sigma}_i \Psi^{\sigma,pd}_j \rangle = \frac{1}{N} \sum_{\mathbf{k},\mathbf{k}'} \langle \Psi^{pd,\sigma}_{\mathbf{k}} \Psi^{\sigma,pd}_{\mathbf{k}'} \rangle \exp(-i\mathbf{k}\mathbf{R}_i + i\mathbf{k}'\mathbf{R}_j), \quad (11)$$

whereas the reverse process (hopping from site j to i) is given by

$$\langle \Psi^{pd,\sigma}_j \Psi^{\sigma,pd}_i \rangle = \frac{1}{N} \sum_{\mathbf{k},\mathbf{k}'} \langle \Psi^{pd,\sigma}_{\mathbf{k}} \Psi^{\sigma,pd}_{\mathbf{k}'} \rangle \exp(-i\mathbf{k}\mathbf{R}_j + i\mathbf{k}'\mathbf{R}_i). \quad (12)$$

Since the hopping integral is a real quantity, the current flow will be proportional to the difference of Eqs. (11) and (12):

$$\langle \Psi^{pd,\sigma}_i \Psi^{\sigma,pd}_j - \Psi^{pd,\sigma}_j \Psi^{\sigma,pd}_i \rangle = \frac{1}{N} \sum_{\mathbf{k},\mathbf{k}'} \langle \Psi^{pd,\sigma}_{\mathbf{k}} \Psi^{\sigma,pd}_{\mathbf{k}'} \rangle \times \{\exp(-i\mathbf{k}\mathbf{R}_i + i\mathbf{k}'\mathbf{R}_j) - \exp(-i\mathbf{k}\mathbf{R}_j + i\mathbf{k}'\mathbf{R}_i)\}. \quad (13)$$

At $T < T^*$ one have the following nonzero expectation values: $\langle \Psi^{pd,\sigma}_{\mathbf{k}} \Psi^{\sigma,pd}_{\mathbf{k}} \rangle$, $\langle \Psi^{pd,\sigma}_{\mathbf{k}+\mathbf{Q}} \Psi^{\sigma,pd}_{\mathbf{k}} \rangle$, and $\langle \Psi^{pd,\sigma}_{\mathbf{k}} \Psi^{\sigma,pd}_{\mathbf{k}+\mathbf{Q}} \rangle$. Since the first one does not contribute, we have

$$\langle \Psi^{pd,\sigma}_i \Psi^{\sigma,pd}_j - \Psi^{pd,\sigma}_j \Psi^{\sigma,pd}_i \rangle = \frac{1}{N} \sum_{\mathbf{k}} \langle \Psi^{pd,\sigma}_{\mathbf{k}+\mathbf{Q}} \Psi^{\sigma,pd}_{\mathbf{k}} \rangle \{\exp[-i(\mathbf{k}+\mathbf{Q})\mathbf{R}_i + i\mathbf{k}\mathbf{R}_j] - \exp[-i(\mathbf{k}+\mathbf{Q})\mathbf{R}_j + i\mathbf{k}\mathbf{R}_i]\} + \frac{1}{N} \sum_{\mathbf{k}} \langle \Psi^{pd,\sigma}_{\mathbf{k}} \Psi^{\sigma,pd}_{\mathbf{k}+\mathbf{Q}} \rangle \times \{\exp[-i\mathbf{k}\mathbf{R}_i + i(\mathbf{k}+\mathbf{Q})\mathbf{R}_j] - \exp[-i\mathbf{k}\mathbf{R}_j + i(\mathbf{k}+\mathbf{Q})\mathbf{R}_i]\}. \quad (14)$$

The order parameter is complex and, thus, it is useful to separate the correlation functions into two parts: $\mathrm{Re}\langle \Psi^{pd,\sigma}_{\mathbf{k}+\mathbf{Q}} \Psi^{\sigma,pd}_{\mathbf{k}} \rangle$ and $\mathrm{Im}\langle \Psi^{pd,\sigma}_{\mathbf{k}+\mathbf{Q}} \Psi^{\sigma,pd}_{\mathbf{k}} \rangle$. It is straightforward to write it further as

$$\langle \Psi_i^{pd,\sigma}\Psi_j^{\sigma,pd} - \Psi_j^{pd,\sigma}\Psi_i^{\sigma,pd}\rangle$$
$$= \frac{2i}{N}\sum_{\mathbf{k}} \mathrm{Im}\langle \Psi_{\mathbf{k}+\mathbf{Q}}^{pd,\sigma}\Psi_{\mathbf{k}}^{\sigma,pd}\rangle\{\cos[\mathbf{k}\mathbf{R}_j-(\mathbf{k}+\mathbf{Q})\mathbf{R}_i]$$
$$-\cos[\mathbf{k}\mathbf{R}_i-(\mathbf{k}+\mathbf{Q})\mathbf{R}_j]\}+\frac{2i}{N}\sum_{\mathbf{k}} \mathrm{Re}\langle \Psi_{\mathbf{k}+\mathbf{Q}}^{pd,\sigma}\Psi_{\mathbf{k}}^{\sigma,pd}\rangle$$
$$\times\{\sin[\mathbf{k}\mathbf{R}_j-(\mathbf{k}+\mathbf{Q})\mathbf{R}_i]-\sin[\mathbf{k}\mathbf{R}_i-(\mathbf{k}+\mathbf{Q})\mathbf{R}_j]\}. \quad (15)$$

If the lattice has a mirror plane symmetry perpendicular to the x and y axis, the integrals over the first Brillouin zone containing $\sin\mathbf{k}\mathbf{R}_{ji}$ vanish. Thus, in the functions $\cos[\mathbf{k}\mathbf{R}_j-(\mathbf{k}+\mathbf{Q})\mathbf{R}_i]-\cos[-\mathbf{k}\mathbf{R}_i+(\mathbf{k}+\mathbf{Q})\mathbf{R}_j]$, and $\sin[\mathbf{k}\mathbf{R}_j-(\mathbf{k}+\mathbf{Q})\mathbf{R}_i]-\sin[-\mathbf{k}\mathbf{R}_i+(\mathbf{k}+\mathbf{Q})\mathbf{R}_j]$ one may leave only the parts $[\cos\mathbf{Q}\mathbf{R}_i-\cos\mathbf{Q}\mathbf{R}_j]\cos\mathbf{k}\mathbf{R}_{ji}$ and $[\sin\mathbf{Q}\mathbf{R}_j-\sin\mathbf{Q}\mathbf{R}_i]\cos\mathbf{k}\mathbf{R}_{ji}$, respectively. Then, the contribution to the current flow along the x axis due to the nearest-neighbor hopping can be calculated to

$$j^{(1)}=\frac{e}{\hbar}t_1\frac{2}{N}\sum_{\mathbf{k}}[\cos\mathbf{Q}\mathbf{R}_i-\cos\mathbf{Q}\mathbf{R}_j]$$
$$\times\mathrm{Im}\langle\Psi_{\mathbf{k}+\mathbf{Q}}^{pd,\sigma}\Psi_{\mathbf{k}}^{\sigma,pd}\rangle\cos\mathbf{k}\mathbf{R}_{ij}$$
$$+\frac{e}{\hbar}t_1\frac{2}{N}\sum_{\mathbf{k}}[\sin\mathbf{Q}\mathbf{R}_j-\sin\mathbf{Q}\mathbf{R}_i]$$
$$\times\mathrm{Re}\langle\Psi_{\mathbf{k}+\mathbf{Q}}^{pd,\sigma}\Psi_{\mathbf{k}}^{\sigma,pd}\rangle\cos\mathbf{k}\mathbf{R}_{ij}. \quad (16)$$

Note, the values of $\mathbf{Q}$ in Eq. (16) differ in the various quadrants of the first Brillouin zone. For example, for $k_x,k_y<0$ and $k_x,k_y>0$ one should take $\mathbf{Q}_1=(\pi,\pi)$ and $\mathbf{Q}_2=(-\pi,-\pi)$, respectively. Then one can show that the second term of Eq. (16) vanishes. Analyzing Eq. (16) we can draw the network patterns for different symmetries of the order parameter (s wave, d wave etc.). Most importantly, for a pure d $_{x^2-y^2}$-wave symmetry of the order parameter one finds $\mathrm{Im}\langle\Psi_{\mathbf{k}+\mathbf{Q}}^{pd,\sigma}\Psi_{\mathbf{k}}^{\sigma,pd}\rangle\sim\cos k_x-\cos k_y$ and the current network pattern is directly mapped to the well-known flux-phase state[17] that is shown in Fig. 1(b). Note that the origin of the coordinate system is arbitrary and the vector $\mathbf{R}_i$ may refer to any point of the unit cell. Of course, the electronic network will be connected to the underlying lattice due to pinning effects. Most likely, two possibilities can be realized. First, when $\mathbf{R}_i=0$, the pinning coincides with the Cu(2) position in the CuO_2 plane and the maximum of the internal magnetic field occurs at the Cu(2) site. Second, if $\mathbf{R}_i=(a/2,a/2)$, the pinning center lies between the Copper sites. For $YBa_2Cu_3O_{7-y}$ this would correspond to the Ba ion acting as a pinning center. In this context, a comparative NMR/NQR experimental study of the fluctuating magnetic fields at Cu(2) and at Ba ion positions are desirable. Furthermore, the pinning associated with one of the out-of-plane oxygen vibrations such as those found in Ref. 18 would yield an interesting example for a stripelike pattern shown in Fig. 1(a).

However, there are other contributions to the network patterns due to the next-nearest-(t_2) and next-next-nearest-(t_3) neighbor hopping. These parameters are needed for a realistic description of the Fermi surface (see, for example, Ref. 19). Their contributions to the orbital currents are given by

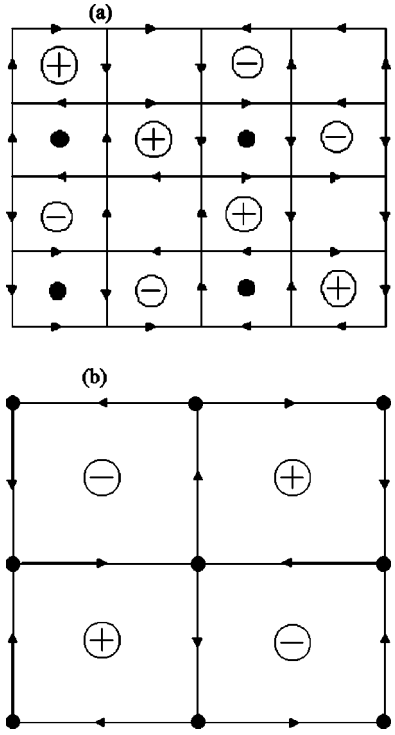

FIG. 1. Network current patterns for the id-CDW state. The black circles correspond to the Copper positions in the CuO_2 plane. In (a), the pinning centers correspond to the oxygen positions whereas in (b) the orbital moments (pinning centers) lie on the Cu(2) position.

$$j^{(2)}=\frac{e}{\hbar}t_2\sqrt{2}\frac{2}{N}\sum_{\mathbf{k}}[\cos\mathbf{Q}\mathbf{R}_i-\cos\mathbf{Q}\mathbf{R}_j]$$
$$\times\mathrm{Im}\langle\Psi_{\mathbf{k}+\mathbf{Q}}^{pd,\sigma}\Psi_{\mathbf{k}}^{\sigma,pd}\rangle\cos\mathbf{k}\mathbf{R}_{ij}+\cdots, \quad (17)$$

for the next-nearest-neighbor hopping and

$$j^{(3)}=\frac{e}{\hbar}t_3\frac{2}{N}\sum_{\mathbf{k}}[\cos\mathbf{Q}\mathbf{R}_i-\cos\mathbf{Q}\mathbf{R}_j]$$
$$\times\mathrm{Im}\langle\Psi_{\mathbf{k}+\mathbf{Q}}^{pd,\sigma}\Psi_{\mathbf{k}}^{\sigma,pd}\rangle\cos\mathbf{k}\mathbf{R}_{ij}+\cdots, \quad (18)$$

for the next-next-nearest-neighbor hopping. Note, in Eq. (17) the indexes i and j refer to the next-nearest neighbors whereas in Eq. (18) i and j refer to the next-next-nearest neighbors.

The required correlation function can be calculated straightforwardly in a mean-field approximation

$$\langle\Psi_{\mathbf{k}+\mathbf{Q}}^{pd,\sigma}\Psi_{\mathbf{k}}^{\sigma,pd}\rangle=\frac{P_{pd}\eta_{\mathbf{k}}}{4}A_+(\mathbf{k},T)$$
$$+\frac{P_{pd}}{2(E_{1\mathbf{k}}^2-E_{2\mathbf{k}}^2)}N_\eta(\mathbf{k})A_-(\mathbf{k},T), \quad (19)$$

where

$$A_{\pm}(\mathbf{k},T)=\frac{1}{E_{1\mathbf{k}}}\tanh\left(\frac{E_{1\mathbf{k}}}{2k_BT}\right)\pm\frac{1}{E_{2\mathbf{k}}}\tanh\left(\frac{E_{2\mathbf{k}}}{2k_BT}\right) \quad (20)$$

and

$$N_{\eta}(\mathbf{k})=\frac{(\varepsilon_{\mathbf{k}}+\varepsilon_{\mathbf{k}+\mathbf{Q}})^2}{2}\eta_{\mathbf{k}}+\Delta_{\mathbf{k}}^2(\eta_{\mathbf{k}}^*+\eta_{\mathbf{k}})+\Delta_{\mathbf{k}}(\varepsilon_{\mathbf{k}+\mathbf{Q}}U_{\mathbf{k}+\mathbf{Q}}^*-\varepsilon_{\mathbf{k}}U_{\mathbf{k}})+\frac{1}{2}(U_{\mathbf{k}}U_{\mathbf{k}}^*+U_{\mathbf{k}+\mathbf{Q}}U_{\mathbf{k}+\mathbf{Q}}^*-2U_{\mathbf{k}}U_{\mathbf{k}+\mathbf{Q}}^*)\eta_{\mathbf{k}}. \quad (21)$$

The energy dispersion is given by the following secular equation:[17]

$$\begin{bmatrix}\varepsilon_{\mathbf{k}}-E & \eta_{\mathbf{k}} & \Delta_{\mathbf{k}} & U_{\mathbf{k}}\\ \eta_{\mathbf{k}}^* & \varepsilon_{\mathbf{k}+\mathbf{Q}}-E & U_{\mathbf{k}+\mathbf{Q}} & -\Delta_{\mathbf{k}}\\ \Delta_{\mathbf{k}} & U_{\mathbf{k}+\mathbf{Q}}^* & -\varepsilon_{\mathbf{k}}-E & -\eta_{\mathbf{k}}^*\\ U_{\mathbf{k}}^* & -\Delta_{\mathbf{k}} & -\eta_{\mathbf{k}} & -\varepsilon_{\mathbf{k}+\mathbf{Q}}-E\end{bmatrix}=0. \quad (22)$$

Note, this secular equation is valid even if the starting Hamiltonian is different from (1) (for example if some additional terms such as interaction with bosonic modes[20] or Cooper-pair hopping are included). Therefore, we will also discuss the possible improvement of the mean-field solution of the *t-J-G* Hamiltonian through the inclusion by including of these terms and making a comparison with available experimental data.

Remarkably, Eq. (22) has a compact solution for the case $|U_{\mathbf{k}}|=|U_{\mathbf{k}+\mathbf{Q}}|$. This allows us to study two possibilities: (a) $U_{\mathbf{k}}=U_{\mathbf{k}+\mathbf{Q}}$ and $U_{\mathbf{k}}$ is real or (b) $U_{\mathbf{k}}^*=U_{\mathbf{k}+\mathbf{Q}}$ and $U_{\mathbf{k}}$ is imaginary. As can be seen from Eq. (20) $A_{\pm}(\mathbf{k},T)$ is a real quantity and one expects that case (b) will be more interesting for studying the formation of orbital currents. In the frame of the *t-J-G* Hamiltonian the equation for the order parameter $U_{\mathbf{k}}$ is

$$U_{\mathbf{k}}=\frac{1}{NP_{pd}}\sum[J_{\mathbf{k}'-\mathbf{k}}+J_{\mathbf{k}'+\mathbf{k}+\mathbf{Q}}-2G_{\mathbf{k}'-\mathbf{k}}]\times\langle\Psi_{\mathbf{k}'}^{\downarrow,pd}\Psi_{-\mathbf{k}'-\mathbf{Q}}^{pd,\downarrow}\rangle, \quad (23)$$

where $P_{pd}=[2+\delta_0]/4$ with δ_0 being the uniform part of the hole distribution per unit cell. At the wave vector $\mathbf{Q}=(\pi,\pi)$ the superexchange integral J_1 does not contribute to the kernel of Eq. (23) and, thus, the absolute value of the order parameter $U_{\mathbf{k}}=iU(T)\cos k_x\cos k_y+\cdots$ will be relatively small.

In the extreme case $U_{\mathbf{k}}=0$, the secular equation leads to the following energy dispersions:

$$E_{1\mathbf{k},2\mathbf{k}}^2=\frac{1}{2}(\varepsilon_{\mathbf{k}}^2+\varepsilon_{\mathbf{k}+\mathbf{Q}}^2)+\Delta_{\mathbf{k}}^2+\eta_{\mathbf{k}}^*\eta_{\mathbf{k}}\pm\frac{1}{2}[(\varepsilon_{\mathbf{k}}^2-\varepsilon_{\mathbf{k}+\mathbf{Q}}^2)^2+4\eta_{\mathbf{k}}^*\eta_{\mathbf{k}}(\varepsilon_{\mathbf{k}}+\varepsilon_{\mathbf{k}+\mathbf{Q}})^2+4\Delta_{\mathbf{k}}^2(\eta_{\mathbf{k}}^*+\eta_{\mathbf{k}})^2]^{1/2}. \quad (24)$$

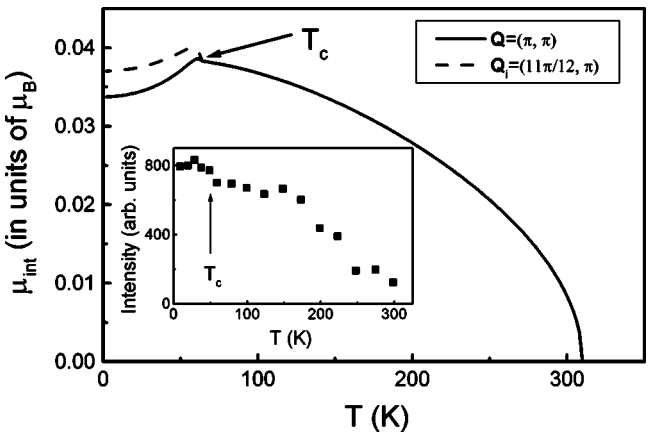

FIG. 2. Calculated intensity of the orbital currents in units of the orbital magnetic moments[18] $\mu_{int}=(j^{(1)}+j^{(2)}+j^{(3)}/2c)a^2$ ($a\approx3.82$ Å is a lattice constant) for two different instability wave vector $\mathbf{Q}=(\pi,\pi)$ (solid curve) and $\mathbf{Q}_i=(\pm11\pi/12,\pi)$ (dashed curve). The inset shows experimental results from Ref. 5.

Here, $\Delta_k=\Delta_0(T)(\cos k_xa-\cos k_ya)$ is a superconducting *d*-wave gap. Combining Eq. (3) and Eq. (5) one deduces that

$$\frac{1}{N}\sum_{\mathbf{k}}\mathrm{Im}\langle\Psi_{\mathbf{k}+\mathbf{Q}}^{pd,\sigma}\Psi_{\mathbf{k}}^{\sigma,pd}\rangle\cos k_xa\approx\frac{d(T)}{J_1+2G_1}P_{pd}. \quad (25)$$

Here J_1, and G_1 are parameters of the superexchange and the screened Coulomb repulsion of the holes at the nearest-neighbor copper sites taken to be 120 meV and 135 meV, respectively. The order parameter $d(T)$ is calculated self-consistently. Using Eq. (25) one immediately sees the simple relation between the current and the $s+id$-CDW order parameter

$$j^{(1)}(T)=\frac{4e}{\hbar}t_1\frac{d(T)}{J_1+2G_1}P_{pd}. \quad (26)$$

The present relation allows us to easily estimate the strength of the orbital currents via the order parameter $d(T)$ or T^*.

For comparison with NS experiments, we show in Fig. 2 the results of our calculations for the case $T^*/T_c\approx5.1$. The temperature dependence of the orbital magnetic moments agrees with the experimental curve in the region $T_c<T<T^*$. The calculated magnitude of the orbital magnetic moments $l_c=[(j^{(1)}+j^{(2)}+j^{(3)})/2c]a^2$ also agrees with the experimental data[5] and is of order $0.03\mu_B$ at $T=T_c$. The corresponding value for the fluctuating magnetic fields produced by the orbital currents $H_{int}\approx[2(j^{(1)}+j^{(2)}+j^{(3)})/cr]$ ($r=2$ Å) at $T<T_c$ are about 180 *G*. This is also in agreement with the values measured by NMR/NQR[9] and μSR[8] experiments. On the other hand, the marked enhancement (''jump'') of the neutron scattering intensity (see, the inset of Fig. 2) below T_c cannot be reproduced by our calculations on a mean-field level.

At present, one can only speculate about the following possible explanations for the observed jump. *First*, this jump may be related to the dynamical nature of the $s+id$-CDW state and its pinning processes. Indeed, as it is seen from the last term of Eq. (24), the energy condensation depends on the

s-wave component of the CDW state if the system enters the superconducting state. Furthermore, the presence of the *s*-wave component makes the condensation energy depend on the phase at $T<T_c$, as is clear from Eq. (24). In our case the *s*-wave component is weak but any additional interaction with the lattice potential will enhance it. Additionally, also the electron-phonon interaction will pin the currents. Then, one expects a marked enhancement of the neutron scattering intesnity below T_c. *Second*, the jump may be related to the fluctuation of the id-CDW instability wave vector around (π,π). This fluctuations can be seen from our calculations of the dynamical charge susceptibility.[12] Indeed, the instability wave vector is not related to (π,π) but rather to some set of the wave vectors along some contour in the first Brillouin zone.[12] For illustration we also have shown in Fig. 2 our results for the temperature dependence of the orbital magnetic moments for the case of the wave vector $\mathbf{Q}_i=(\pi, \pm 11\pi/12)$ that lies in this contour.[12]*Third*, the jump of the neutron scattering intensity might also result from the appearance of the order parameter $U_{\mathbf{k}}$ below T_c. However, in the frame of a mean-field solution of the *t*-*J*-*G* Hamiltonian, this order parameter was found to be small. Thus, calculations beyond the standard mean-field level and the *t*-*J*-*G* model would be desirable.

Finally, we would like to discuss the influence of the competition between id-CDW and *d*-wave superconductivity on the general phase diagram that is shown in Fig. 3 as a function of doping concentration. Note, our phase diagram looks similar to the one proposed in Ref. 1 with some important differences. In particular, the boundary of the id-CDW state (DDW in the terminology of Ref. 1) after crossing the superconducting dome moves to the left, while in Ref. 1 it goes to the right (see, Fig. 1 of Ref. 1). In our case, the reason for this behavior is very clear: The orbital currents result from the id-CDW state that describes the ''pairing'' of the quasiparticles with parallel spins while Cooper-pairing requires them to be antiparallel. Therefore, in the regime of coexistence of id-CDW and *d*-wave superconductivity the latter will try to push the orbital currents out. This behavior was found earlier in Ref. 20 and experimentally by tunneling spectroscopy.[21] Therefore, in order to understand the role played by id-CDW state in the cuprates the details of competition between pseudogap and superconductivity have to be studied more in detail experimentally. For example, further experimental studies are required in order to verify the orientation of the observed magnetic moments. According to Ref. 5 they are aligned along the *c* axis (this agrees with the id-CDW scenario) whereas the polarization of the magnetic moments reported by other group[6] lies in the copper-oxygen plane.

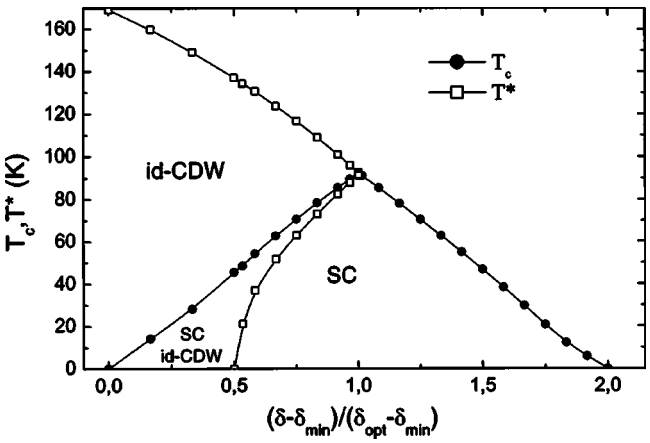

FIG. 3. Calculated phase diagram for the competition between id-CDW state and *d*-wave superconductivity in the *t*-*J*-*G* model. The doping axis is normalized with respect to optimal doping (i.e., the concentration that corresponds to the maximum of superconducting transition temperature, T_c) and to δ_{min} and δ_{max}, where one finds both superconducting order parameters to be zero.

In summary, in the frame of *t*-*J*-*G* model we analyze the regime of coexistence of *d*-wave superconductivity and the $s+id$-CDW phase. We obtain a microscopic expression for the circulating orbital current via the anomalous correlation function. The simple relation between the strength of the currents (or orbital magnetic moments) and the id-CDW order parameter was established. The temperature dependence of the orbital magnetic moments (and the internal magnetic fields they produce) and their order of magnitude are in agreement with experimental data. However, some important details remain controversal and probably are missed in the one-band *t*-*J*-*G* model. We emphasize the importance of NMR experiments that are able to analyze the actual temperature and doping ranges of the competition between $s+id$-CDW and *d*-wave superconductivity.

We are thankful for stimulating discussions with A. Dooglav, A. Rigamonti, J. Roos, D. Manske, C. Joas, and D. K. Morr. This work was supported by the Swiss National Foundation (Grant No. 7SUOJ062258), Russian Scientific Council on Superconductivity (Project No. 98014-3), and partially by the CRDF (Grant No. REC-007). I.E. was supported by the Alexander von Humboldt Foundation.

[1] S. Chakravarty, R.B. Laughlin, D.K. Morr, and Ch. Nayak, Phys. Rev. B **63**, 094503 (2001).

[2] S. Tewari, H.-Y. Kee, Ch. Nayak, and S. Chakravarty, Phys. Rev. B **64**, 224516 (2001).

[3] S. Chakravarty, H.-Y. Kee, and Ch. Nayak, Int. J. Mod. Phys. B **15**, 2901 (2001).

[4] A. Kaminski, S. Rosenkranz, H.M. Fretwell, J.C. Campuzano, Z. Li, H. Raffy, W.G. Cullen, H. You, C.G. Olson, C.M. Varma, and H. Höchst, Nature (London) **416**, 610 (2002).

[5] H.A. Mook, P. Dai, and F. Dogan, Phys. Rev. B **64**, 012502 (2001).

[6] Y. Sidis, C. Ulrich, Ph. Bourges, C. Bernhard, C. Niedermayer, L.P. Regnault, N.H. Andersen, and B. Keimer, Phys. Rev. Lett. **86**, 4100 (2001).

[7] J.A. Hodges, Y. Sidis, Ph. Bourges, I. Mirebeau, M. Hennion, and X. Chaud, Phys. Rev. B **66**, 020501 (2002).
[8] J.E. Sonier, J.H. Brewer, R.F. Kiefl, R.I. Miller, G.D. Morris, C.E. Stronach, J.S. Gardner, S.R. Dunsiger, D.A. Bonn, W.N. Hardy, R. Liang, and R.H. Heffner, Science **292**, 1692 (2001); A. Kanigel, A. Keren, Y. Eckstein, A. Knizhnik, J.S. Lord, and A. Amato, Phys. Rev. Lett. **88**, 137003 (2002); R.I. Miller, R.F. Kiefl, J.H. Brewer, J.E. Sonier, J. Chakhalian, S. Dunsiger, G.D. Morris, A.N. Price, D.A. Bonn, W.N. Hardy, and R. Liang, *ibid.* **88**, 137002 (2002).
[9] M.V. Eremin and A. Rigamonti, Phys. Rev. Lett. **88**, 037002 (2002).
[10] M.V. Eremin, Yu.A. Sakhratov, A.V. Savinkov, A.V. Dooglav, I.R. Mukhamedshin, and A.V. Egorov, Pis'ma Zh. Éksp. Teor. Fiz. **73**, 609 (2001) [JETP Lett. **73**, 540 (2001)].
[11] A.V. Dooglav, M.V. Eremin, Yu.A. Sakhratov, and A.V. Savinkov, Pis'ma Zh. Éksp. Teor. Fiz. **74**, 108 (2001) [JETP Lett. **74**, 103 (2001)].
[12] M. Eremin, I. Eremin, and S. Varlamov, Phys. Rev. B **64**, 214512 (2001).
[13] F.C. Zhang and T.M. Rice, Phys. Rev. B **37**, 3759 (1988).
[14] M.V. Eremin, S.G. Solovjanov, and S.V. Varlamov, Zh. Eksp. Teor. Fiz. **112**, 1763 (1997) [JETP **85**, 963 (1997)].
[15] N.M. Plakida, R. Hayn, and J.L. Richard, Phys. Rev. B **51**, 16 599 (1995).
[16] J.M. Harris, Z.-X. Shen, P.J. White, D.S. Marshall, M.C. Schabel, J.N. Eckstein, and I. Bozovic, Phys. Rev. B **54**, 15 665 (1996).
[17] T.C. Hsu, J.B. Marston, and I. Affleck, Phys. Rev. B **43**, 2866 (1991).
[18] A. Bianconi, N.L. Saini, A. Lanzara, M. Missori, T. Rossetti, H. Oyanagi, H. Yamaguchi, K. Oka, and T. Ito, Phys. Rev. Lett. **76**, 3412 (1996).
[19] M.R. Norman, Phys. Rev. B **61**, 14 751 (2000).
[20] M.V. Eremin and I.A. Larionov, Pis'ma Zh. Éksp. Teor. Fiz. **68**, 583 (1998) [JETP Lett. **68**, 611 (1998)].
[21] T. Ekino, Y. Sezaki, and H. Fujii, Phys. Rev. B **60**, 6916 (1999).